Stimulus-induced Critical Point

Mechanism for Electrical Initiation of Reentry in Normal Canine Myocardium

David W. Frazier, Patrick D. Wolf, J. Marcus Wharton, Anthony S. L. Tang, William M. Smith, and Raymond E. Ideker
Departments of Medicine and Pathology, Duke University Medical Center, Durham, North Carolina 27710

Abstract

The hypothesis was tested that the field of a premature (S2) stimulus, interacting with relatively refractory tissue, can create unidirectional block and reentry in the absence of nonuniform dispersion of recovery. Simultaneous recordings from a small region of normal right ventricular (RV) myocardium were made from 117 to 120 transmural or epicardial electrodes in 14 dogs. S1 pacing from a row of electrodes on one side of the mapped area generated parallel activation isochrones followed by uniform parallel isorecovery lines. Cathodal S2 shocks of 25 to 250 V lasting 3 ms were delivered from a mesh electrode along one side of the mapped area to scan the recovery period, creating isogradient electric field lines perpendicular to the isorecovery lines. Circus reentry was created following S2 stimulation; initial conduction was distant from the S2 site and spread towards more refractory tissue. Reentry was clockwise for right S1 (near the septum) with top S2 (near the pulmonary valve) and for left S1 with bottom S2; and counterclockwise for right S1 with bottom S2 and left S1 with top S2. The center of the reentrant circuit for all S2 voltages and coupling intervals occurred at potential gradients of 5.1±0.6 V/cm (mean±standard deviation) and at preshock intervals 1±3 ms longer than refractory periods determined locally for a 2 mA stimulus. Thus, when S2 field strengths and tissue refractoriness are uniformally dispersed at an angle to each other, circus reentry occurs around a "critical point" where an S2 field of ~ 5 V/cm intersects tissue approximately at the end of its refractory period.

Introduction

The mechanism for the electrical induction of fibrillation has been attributed to nonuniform dispersion of recovery following stimulation during the relative refractory period (1–5). Recovery may be dispersed uniformly or nonuniformly (6). When dispersed uniformly, it changes approximately the same amount over a given distance throughout the region, i.e., it has a constant gradient. When dispersed nonuniformly, it changes at different rates at different places and may change rapidly over a small distance so that one site remains refractory long after a nearby site has recovered. Nonuniform dispersion of recovery may be present due to intrinsic differences in refractory periods of individual cells or to asymmetric spread of activation with accompanying differences in recovery times (1, 7). According to traditional theory, premature stimulation results in temporary unidirectional conduction block in areas of later recovery with the spread of activation towards areas of earlier recovery, thus favoring the development of reentry and ventricular fibrillation. Although some have alluded to the "extra inhomogeneity" induced by the electrical shock (8), the underlying nonuniform dispersion of recovery has usually been assumed to be present before the application of the electrical stimulus. The fibrillation threshold decreases as the underlying dispersion is increased by premature stimulation, beta adrenergic stimulation, ischemia, infarction, or various drugs, thereby lending support to this hypothesis (1–4, 7–11).

Other evidence suggests, however, that nonuniform dispersion of recovery is not crucial for the induction or maintenance of reentry. In small regions of normal myocardium, the underlying dispersion of recovery after basic drive beats is small (2, 4, 6, 12). The induction of fibrillation in normal myocardium by single premature stimuli usually requires currents of 10–20 mA or more (9, 11, 13–17), a value larger than that required to excite most relatively refractory tissue. Lower stimulus currents require additional measures to increase the electrical instability, such as ischemia, before fibrillation can be induced. Spach et al. (18) have shown that different safety factors along and across fibers can lead to unidirectional block during premature stimulation. Anisotropic conduction velocity alone can sustain reentrant circuits, with the long axis of block oriented parallel to the local fiber orientation (12, 19).

The purpose of this study was to test a different hypothesis for the mechanism of the induction of reentry in normal myocardium via suprathreshold electrical stimulation: that interaction of a certain strength of S2 shock field with tissue of a certain refractoriness creates reentry at the point where the critical values of S2 field strength and refractoriness intersect, i.e., the "critical point," without requiring refractoriness to be dispersed nonuniformly (6, 20–22).

Methods

Surgical procedure

14 mongrel dogs weighing 19 to 28 kg were anesthetized with pentobarbital (30–35 mg/kg) (23) and succinylcholine (1 mg/kg). Each was intubated with a cuffed endotracheal tube and ventilated with 30–40% oxygen. Ringer's lactate was continuously infused and supplemented with potassium chloride, sodium bicarbonate, and calcium chloride when indicated. Via a separate intravenous line, pentobarbital was infused at a rate of ~ 0.05 mg/kg per min throughout the experiment. The dose of pentobarbital was adjusted according to the depth of anesthesia as assessed by shivering, eyelid reflexes, and pedal reflexes (23). Succinylcholine at a bolus dose of 0.5 mg/kg was given no more than once per hour to decrease muscle contractions induced by the electric shocks. A catheter was inserted into the femoral artery, and the

Address reprint requests to Dr. Frazier, P. O. Box 3140, Duke University Medical Center, Durham, NC 27710.

Received for publication 14 April 1988 and in revised form 22 August 1988.

J. Clin. Invest.

0021-9738/89/03/1039/14 $2.00
Volume 83, March 1989, 1039–1052

systemic blood pressure was continuously displayed on an oscilloscope. Blood was withdrawn to determine the pH, Po_2, Pco_2, CO_2 content, base excess, and bicarbonate, sodium, potassium, and calcium concentrations. Normal metabolic status was maintained throughout the study by taking blood samples every 30–60 min and by correcting any abnormal value.

The chest was opened through a median sternotomy, and the heart was suspended in a pericardial cradle. The sinus node was crushed to allow stable pacing rates. In three dogs a fixed array of 40 plunge needles (120 electrodes) was inserted into the right ventricular free wall, allowing transmural recordings from subendocardial, midmyocardial, and subepicardial planes (Fig. 1 *A*) (24). In the remaining 11 dogs an array of 117 bipolar electrodes was sutured to the epicardium (Fig. 1 *B*). Wire mesh electrodes were sutured to the epicardial surface at the top, bottom, and/or left sides of the electrode array. Eight epicardial pacing wires, 4- to 5-mm apart, were sutured parallel to and within 3 mm of the left and right sides of the electrode array.

Stimulation protocol

Baseline cathodal S1 pacing using a 10-mA constant current source was performed simultaneously from the eight pacing wires on one side of the array using the tongue as the anode. An S1 strength of 10 mA was chosen because lower currents often failed to capture some of the eight pacing sites. A train of 10 S1s was given at a cycle length of 300–350 ms, and the pattern of activation following the tenth S1 stimulus was analyzed to verify the presence of uniform and parallel activation wavefronts. If parallel isochronal lines were not created, additional pacing wires were placed along the row of eight pacing wires at regions of late activation and determination of the S1 activation pattern was repeated.

After verification of a stable parallel S1 activation pattern, recovery periods were determined at 24 to 44 recording electrode sites. The time of recovery of excitability after the basic response (V1) following the tenth S1 stimulus was successively determined at each electrode site by delivering a premature cathodal stimulus (S2) at an intensity of 2 mA and a duration of 3 ms. S1-S2 intervals were decremented in steps of 2 or 3 ms. The shortest S1-S2 interval that produced a propagated response to recording electrodes 3.8 mm away was taken as the recovery period duration for that electrode site (25). The refractory period was defined as the V1-S2 interval for that electrode site. To obtain a measure of the average tissue refractoriness within the mapped area, the mean of the refractory periods at 24–44 recording electrode sites for each dog was determined and called the mean refractory period. Refractory period measurements were repeated once or twice during the course of each study.

After determination of the recovery periods, unipolar cathodal S2 shocks (25–250 V) were delivered to each wire mesh electrode following the last S1 stimulus, with the anode attached to the metal chest wall dividers. The activation patterns after these S2 stimuli were mapped. Initially, diastolic shocks of selected voltages, 10 ms in duration, were delivered from each mesh electrode to allow determination of the potential gradient distribution. S2 stimuli 3 ms in duration were then delivered at decremental or incremental S1-S2 intervals of 3–5 ms to span the recovery periods of the tissue under the electrode array. Although all combinations of S1 and S2 locations plus all voltage ranges and S1-S2 interval ranges were not possible within individual dogs, all dogs received S1 pacing from the right (septal) side of the electrode array and S2 shocks from the top (nearest the pulmonary valve) with S2 voltages that produced potential gradients of 4–6 V/cm near the center of the electrode array. In addition, a range of S2 voltages producing large or small potential gradient ranges within the array was also tested. In eight dogs the S1 and S2 locations were from neighboring sides to create S1 activation patterns perpendicular to S2 field strength patterns. In the remaining dogs the activation patterns following both perpendicular and parallel interactions of the isorecovery and isogradient lines were mapped. 5–15 fibrillation episodes per dog were analyzed on-line to allow verification of the activation patterns. A specially designed defibrillator (Intermedics, Inc.) with a capacitance of 900 μF was used to deliver the S2 shocks. Waveforms were monitored on a waveform analyzer (Data Precision) to ensure accurate and reproducible delivery of a desired voltage. For shocks that initiated fibrillation, defibrillation was achieved within 10 to 15 s using internal defibrillator paddles applied over the pericardium. There was a mean of 21±10 fibrillation-defibrillation episodes per dog. A minimum of 5 min and usually 10–15 min elapsed between fibrillation episodes.

Data acquisition

A computer-assisted mapping system capable of simultaneously recording from 128 channels was used to record both the stimulus potentials and the activation complexes (26). Activations before and after the S2 stimulus were filtered from 0.1 to 500 Hz and digitized at a rate of 1,000 samples per second. 15 ms before the S2, a 1,000:1 voltage attenuator was switched in front of each channel, and each amplifier gain was switched to a value that allowed adequate potential field recording. During the period of attenuated recording the bandwidth of all amplifiers was DC to 500 Hz. Immediately after the S2, the attenuators were switched out and the amplifiers returned to the electrogram recording state (27). This allowed the detection of activation complexes 5–7 ms after the end of high voltage stimuli. Surface ECG leads I, II, and III were recorded simultaneously, and all data were stored on video tape for off-line analysis (28). The recordings from each channel were subsequently displayed on a Tektronix 4014 graphics terminal to allow measurement of S2 stimulus potentials and detection of activation times before and after the S2 stimulus.

Tissue examination

At the end of each study the dog was sacrificed by electrically induced ventricular fibrillation, and the portion of myocardium under the electrode array was removed. The endocardium under the electrode array was immediately stained with Lugol's solution to demonstrate the Purkinje fibers. The portion of myocardium was then fixed with 10% buffered formalin for at least 48 h.

For the three dogs with intramural recordings, serial sections of tissue were taken transmurally at 0.5-mm intervals parallel to the epicardial surface. For the 11 dogs in which the epicardial electrode array was used, sections were taken at 0.5-mm intervals for the first 2 mm from the epicardium and then at 1-mm intervals until the endocardium was reached. The sections were stained with hematoxylin-eosin and the fiber orientation determined relative to the horizontal axis of the electrode array (29). The fiber orientation was used in the calculation of potential gradients, current densities, and energies. For the epicardial array, only the epicardial fiber orientation was used in the calculations.

Data analysis

Calculation of potential gradients. The stimulus potential was defined as the unipolar potential recorded by an electrode during the stimulation pulse relative to the left hind leg potential. The 10-ms baseline immediately preceding each stimulus was used as the zero value in the measurement of stimulus potentials for each recording electrode. The calculation of potential gradients, current densities, and energies from the measured stimulus potentials has been previously described (29). Briefly, a finite element model was used to incorporate the anisotropies of myocardial fiber orientation and of conductivity. In four dogs from preliminary studies in which the basic techniques of the stimulation protocol were developed, plus three dogs included in the data analysis, the plunge electrode array was used to record transmural potentials during the S2 shocks. The component of the potential gradient perpendicular to the epicardial surface at the level of the midwall accounted for 9.7% of the total magnitude of the potential gradient for the entire range of potential gradients created by the 25- to 250-V S2 shocks. In the region of the reentrant sites, i.e., the critical points, the transmural component was < 5% of the total magnitude. For the 11 dogs with the epicardial electrode array, therefore, the measured epicardial potentials were used to compute the field strength parameters with the assumption that, since the transmural component was small, the calcu-

lated parameters were approximately equivalent to those obtained from the plunge electrode array.

Analysis of recordings. For bipolar recordings, the time of activation was taken as the time of the fastest slope for biphasic waveforms and the time of the absolute peak magnitude for monophasic and triphasic waveforms (30). Isochronal maps were drawn for all activations analyzed (31). Regions in which conduction velocity would be less than 0.1 m/s if conduction were present are designated as exhibiting conduction block and are indicated on the maps by block lines. The border representing the transition between successive activation maps is defined as the frame line. Frame lines are the break points between maps and are necessary to represent the dynamic continuous activation sequence of reentry by a series of static discrete isochronal maps. The preshock interval at each recording electrode site is defined as the time from S1 activation at that site to the S2 shock, or S2 minus the local V1.

Statistical methods. Data were analyzed using the paired t test and linear regression (32). $P < 0.05$ was interpreted as being significant. Values are given as mean±SD.

Results

Isogradient and isorecovery patterns

The principal goal of the experimental design (Fig. 1) was to create parallel isorecovery lines following S1 pacing and parallel isogradient lines during S2 shocks, allowing perpendicular or parallel interaction of these lines depending on the locations of the S1 and S2 electrodes. Thus, the initial step in the experiment was the creation and on-line verification of these parallel lines.

Instead of a point source, which would have generated elliptical isopotential lines, the S2 shocks were delivered from a long mesh electrode extending beyond both sides of the mapped area to create parallel isopotential lines (Fig. 2 *A*). The isogradient lines calculated from these stimulus potentials were approximately parallel to the top and bottom sides of the mapped area, with gradient magnitudes for the example shown in Fig. 2 *B* ranging from 13.6 to 2.7 V/cm with 6 V/cm appearing approximately in the middle of the array. The S2 stimuli from other mesh electrodes and in other dogs produced similar parallel distributions of potential gradients.

The activation patterns during S1 stimulation were uniform and nearly parallel in all cases (Figs. 3, 9 *A*, 10 *A*). The recovery periods at 24 to 44 sites (a mean of 33 per dog) were determined using 2 mA premature stimuli (Fig. 3). These 2-mA stimuli were typically four to six times diastolic threshold for four to eight random sites tested during each experiment. Nearly parallel isorecovery lines were created closely approximating the S1 isochronal activation lines (Fig. 3). Although slightly more heterogeneity in the recovery periods was occasionally seen than in Fig. 3 (see Fig. 9 *A*), the refractory periods were approximately the same at all electrode sites within each dog; the mean of the standard deviations of the refractory periods for all dogs was 2.7±0.8 ms with a range of 1 to 4 ms. Thus, a minimum of inhomogeneous refractoriness existed.

The approximate boundary of the region of myocardium directly excited by the S2 shock was determined from the distribution of refractoriness following S1 stimulation, from the S1-S2 interval at which the S2 shock was delivered, and from the patterns of activation following the S2 shock. At a given S1-S2 interval, if a uniform potential gradient field could have been created over the entire array that was equivalent to the field produced locally by the 2-mA point stimulus used during determination of the recovery periods, then all of the area with recovery periods less than or equal to this S1-S2 interval

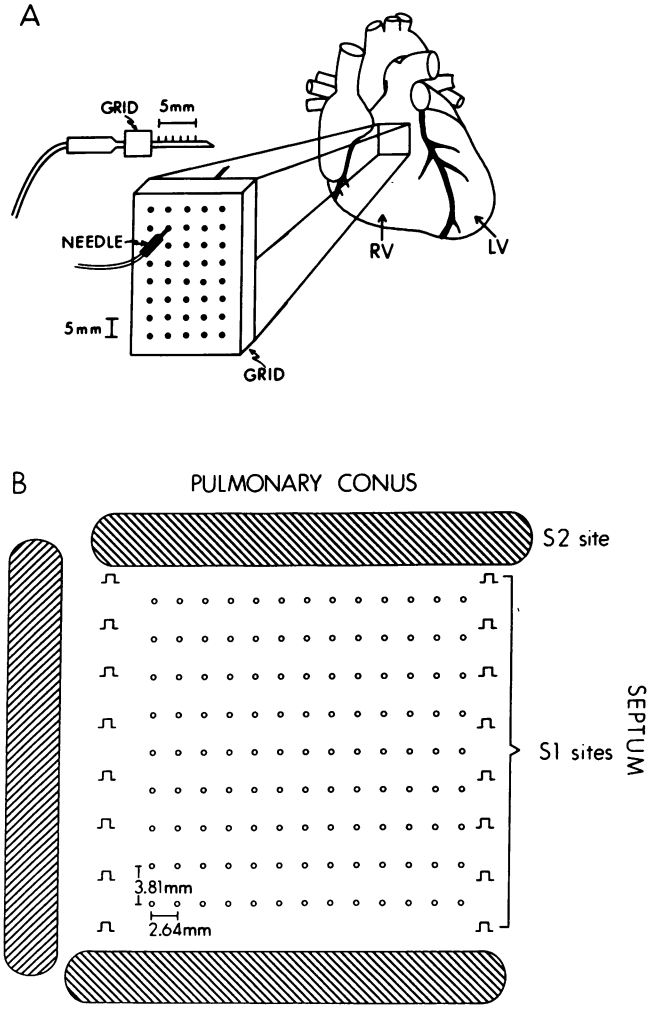

Figure 1. Transmural and epicardial electrode arrays. (*A*) Transmural array. 40 plunge electrodes held within a plastic array were inserted into the right ventricular outflow tract and free wall, allowing recording from 120 transmural bipolar electrodes in the subendocardial, midmyocardial, and subepicardial planes of myocardial tissue. The top of the array was located within 2 cm of the pulmonary valve and the right side parallel to and within 1 to 2 cm of the left anterior descending coronary artery. Stainless steel mesh electrodes, 4.5 × 1 cm (as shown in *B*), were sutured to the epicardial surface along the top and bottom of the array. S2 stimuli were delivered from one of the two mesh electrodes. A row of eight epicardial pacing wires (as shown in *B*) was sutured along the right and left sides of the array. S1 stimuli were delivered from one of the two rows of pacing wires. (*B*) Epicardial array. Epicardial recordings were obtained from an array of 117 surface bipolar electrodes (*open circles*) held within an epicardial array placed in approximately the same position on the right ventricle as the transmural array. The stainless steel mesh electrodes were sutured to the epicardial surface along the top (labeled "S2 site"), bottom, and/or left sides of the array, and epicardial pacing wires were placed along the right (labeled "S1 sites") and left sides of the array. In the remaining figures the sites of the pacing wires and mesh electrodes are designated as S1 and S2, respectively.

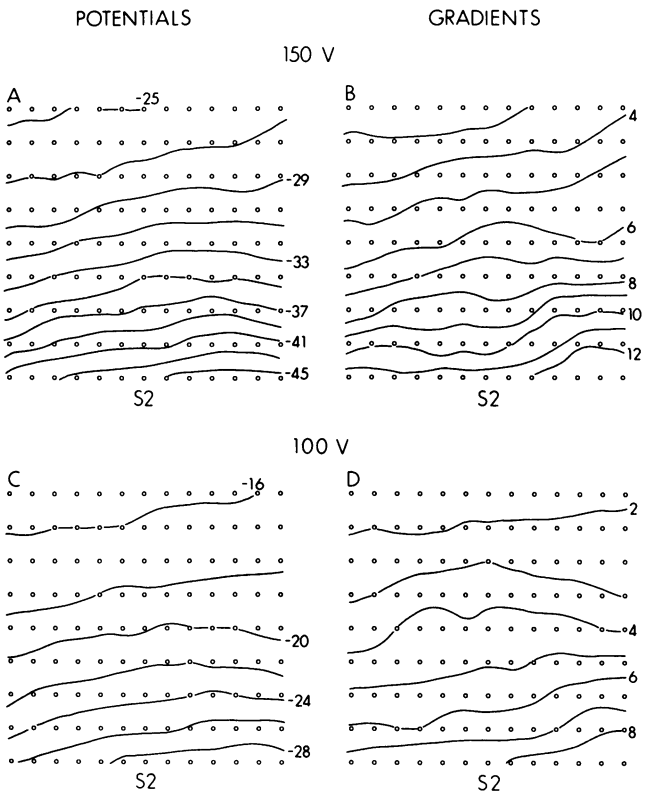

Figure 2. Stimulus potentials and potential gradients. (*A* and *B*) The epicardial stimulus potentials and potential gradients, respectively, for a unipolar cathodal shock of 150 V from the bottom mesh electrode. Isopotential and isogradient lines approximately parallel to the bottom of the array are created, with gradients of 6 V/cm occurring near the middle of the array. The isopotential values are given in volts (V), and the isogradient values in volts per centimeter. (*C* and *D*) The potentials and gradients for a 100-V S2. Gradients of 6 V/cm occur closer to the S2 site than for the 150 V S2. Figs. 2 through 7 are taken from the same animal.

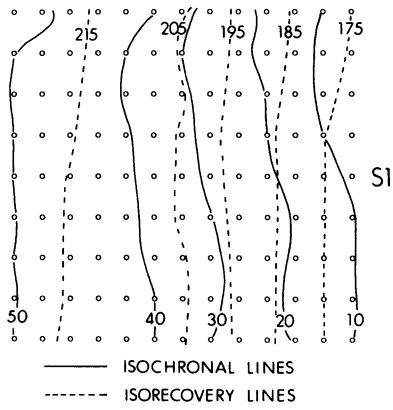

Figure 3. S1 activation and isorecovery patterns. The row of eight epicardial pacing wires was tied together as a single source (S1) and paced at 10 mA. Approximately parallel isochronal lines (*solid lines*) are created by S1 pacing, with conduction velocities of 0.5 to 0.7 m/s. The wider isochronal spacing to the left of the array, distant from the S1 site, probably indicates a sizable endocardial to epicardial component to the spread of activation in that region (24). The recovery periods (*dashed lines*) were calculated at 32 electrode sites evenly spaced across the array for this example. The refractory periods were similar at all electrode sites (166±3 ms), indicating minimal inhomogeneous refractoriness. The mean epicardial fiber orientation under the array, in this case was 24±5 degrees with respect to the horizontal.

should have been directly excited by the field of the S2 shock. The S2 shocks delivered from the mesh electrodes, however, generated a range of potential gradients that presumably spanned the local field strength created by the 2-mA point stimulus. The isogradient diastolic threshold is known to be 0.8 to 1.2 V/cm (29, 33). Thus, potential gradients of 4–6 V/cm are approximately five times larger than the gradient at the diastolic threshold, similar to the 2-mA stimuli, which are approximately five times the diastolic threshold. In regions with potential gradients slightly higher or lower than 4–6 V/cm, the region directly excited by the S2 shock can be presumed to be slightly greater or lesser, respectively, than predicted from the S1-S2 interval and the recovery periods. Therefore, the border of the region directly excited by the S2 field should not be exactly parallel to the isorecovery lines, but should be slightly tilted, the border being closest to the S1 electrodes where the potential gradient field is weakest, i.e., farthest from the S2 electrode. Identification of the directly excited border is straightforward in those regions where activation conducts away from this border after the shock; the border is coincident with the frame line of the first activation map (Fig. 4 *A*). In regions where activation does not conduct away from the border after the shock, the area directly excited by the S2 shock is not definitely known. The affected area is assumed to depend on the pattern of isorecovery lines, and, because of large field strengths in this region, to tilt slightly away from the S1 site as shown by the hatched area in Fig. 4 *A*. Even though the activation times in the hatched area (85 to 156 ms) are the first recorded in this region following the shock, they are assumed to be the second activation associated with the shock since the first was direct excitation caused by the S2 shock itself.

Activation patterns for perpendicular isorecovery and isogradient lines

Alteration of S1 and S2 sites. Reentrant activation leading to ventricular fibrillation was induced following all four perpendicular interactions of the isorecovery and isogradient lines: right S1 with bottom S2 (Figs. 4 and 5), right S1 with top S2 (Fig. 6 *A*), left S1 with top S2 (Fig. 6 *B*), and left S1 with bottom S2 (Fig. 6 *C*). To allow comparisons of the different S1 and S2 sites, Figs. 2–7 are taken from the same dog. For the three dogs in which transmural recordings were obtained (see below), the patterns of activation on the subepicardium did not differ substantially from the subendocardial and midmyocardial patterns, nor were the subepicardial patterns substantially different from those obtained using the epicardial array. Because greater detail in the reentrant circuits was obtained using the more closely spaced epicardial electrodes, the patterns of activation leading to ventricular fibrillation are predominantly illustrated with data obtained from the epicardial array.

Fig. 4 shows reentrant patterns for the combination of right S1 (isogradient pattern shown in Fig. 2 *B*) and bottom S2 (isorecovery pattern shown in Fig. 3), with selected electrode recordings shown in Fig. 5. Initial poststimulus propagation occurs distant from the S2 site at the top of the array, with activation times of 8–14 ms occurring along the frame line marking the border of the directly excited region. Activation fronts then conduct towards the S2 site around a region of apparent conduction block (hatched line). No activation front conducts away from the directly excited boundary near the S2 site; this region is excited via the activation front propagating

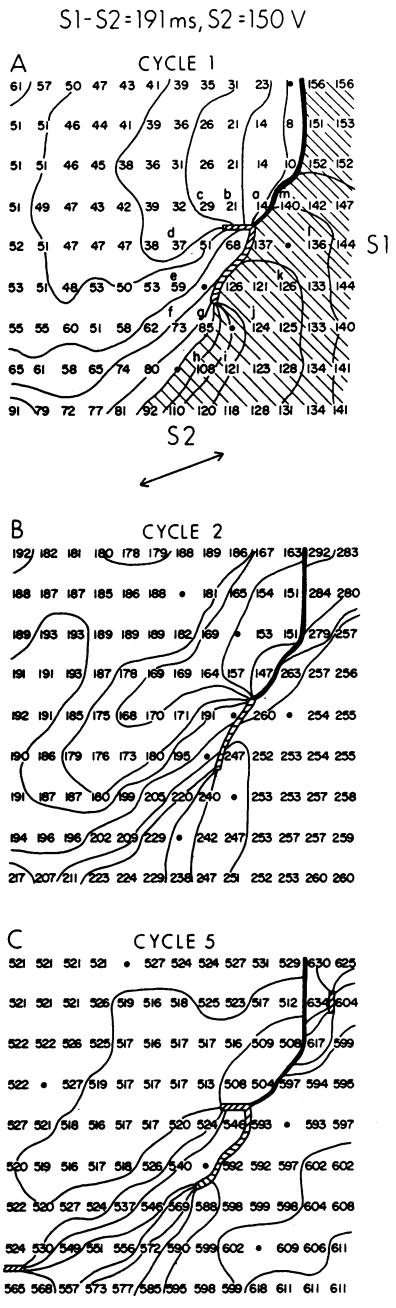

Figure 4. Activation patterns for perpendicular isorefractory and isogradient lines. The patterns of activation following S1 pacing from the right and S2 shock from the bottom are shown in *A* (cycle 1), *B* (cycle 2), and *C* (cycle 5). Activation times, shown in milliseconds, are measured from the start of the 3-ms S2 shock. Solid dots represent sites of inadequate recordings. The solid line represents the transition between successive activation maps and is called a "frame line." The hatched line represents a zone of conduction block and is called a "block line." Isochrones are at 10-ms intervals. The doubled-headed arrow for this figure and for Figs. 6 and 7 represents the mean epicardial fiber orientation in the area of conduction block, in this case 21 degrees with respect to the horizontal. (*A*) The initial activation pattern following the S2 shock at an S1-S2 interval of 191 ms and an S2 strength of 150 V. The letters *a* to *m* represent the electrode recordings shown in Fig. 5. The hatched area indicates the region assumed to be directly excited by the S2 shock field. Earliest postshock activation occurs distant from the S2 site, with no early activation wavefronts conducting away from the directly excited region located between the S2 site and the critical point, i.e., the point where the activation front blindly ends at the junction between the frame line and the block line. A counterclockwise reentrant circuit is formed around the region containing the critical point and the line of block. The potential gradient equals 5.8 V/cm and the preshock interval equals 171 ms at the critical point (critical refractory period = 169 ms). (*B*) The second cycle of the reentrant pattern. No slow conduction occurs at the frame line between the first and second reentrant cycles. The activation pattern is similar to the first cycle except that the circuit time is decreased to 122 ms. (*C*) The fifth cycle of the reentrant pattern. The reentrant pattern is similar to the previous cycles; however, the total circuit time has further decreased to 101 ms.

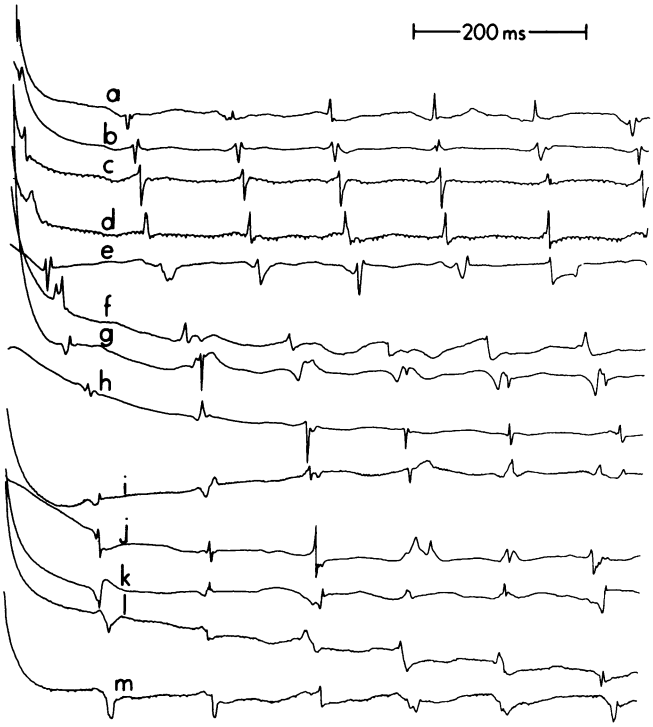

Figure 5. Electrode recordings around the critical point. Bipolar electrode recordings are shown for the sites labeled *a* through *m* in Fig. 4 *A* beginning 3 ms after the end of the S2 shock. The S1 activations and S2 shock are not shown.

away from the directly excited boundary distant from the S2 site. Conduction velocity is rapid in the first half of the reentrant circuit, ~ 0.5 m/s (with wide variation). Slow conduction, 0.15 to 0.25 m/s, occurs in the reentrant circuit over a 6- to 10-mm region near the S2 site. This region contains the assumed boundary of direct excitation. Once past this region, the activation front accelerates and forms a complete reentrant circuit. Slow conduction is not present near the frame line between cycles 1 and 2. This pattern is essentially repeated for the first 10 cycles (Figs. 4, *B* and *C*).

A critical point occurs, above which an activation front conducts away from the directly excited boundary and below which it does not. Activation spirals around the region encompassing the critical point and the line of conduction block, forming a reentrant pathway. The local potential gradient during the S2 shock at the four electrodes surrounding the critical point in Fig. 4 *A* is 5.8 V/cm. The preshock interval is 171 ms as compared to the critical refractory period (the mean of the refractory periods at the four electrodes surrounding the critical point) of 168 ms. Thus, counterclockwise circus reentry is created following perpendicular interaction of uniform isorecovery and isogradient lines for S1 on the right and S2 at the bottom, with a critical point at a potential gradient of slightly < 6 V/cm and at a preshock interval approximately equal to the critical refractory period.

Moving the S2 site to the top of the array produces a similar reentrant pattern (Fig. 6 *A*), except the reentrant pattern is clockwise and is shifted in phase by ~ 180 degrees, with earliest activation occurring at the bottom of the array. Slow conduction again occurs near the S2 site but over a slightly larger area and with a slightly faster velocity than in the previous example.

Left S1 with top S2 produces counterclockwise reentry (Fig. 6 *B*), while left S1 with bottom S2 produces clockwise

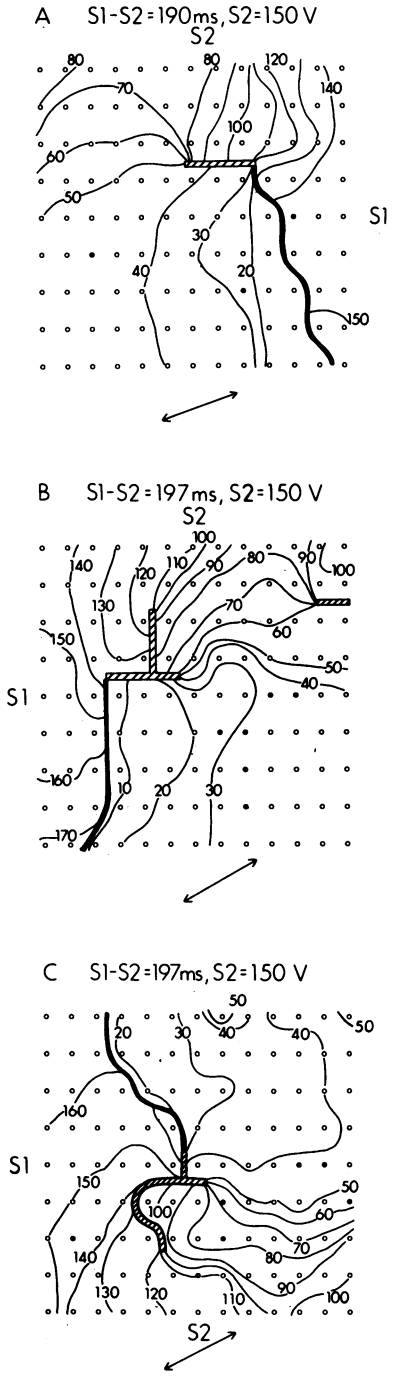

Figure 6. Effect of locations of S1 and S2 on direction of reentrant circuits. (*A*) The first cycle of reentry following a 150 V S2 at an S1-S2 interval of 190 ms is shown with S2 at the top and S1 towards the septum. Earliest activation occurs distant from the S2 site, with activation wavefronts then conducting around a line of block with slow conduction near the S2 site. A clockwise reentrant circuit is formed, versus the counterclockwise circuit with S2 at the bottom (Fig. 4 *A*). In addition, the reentrant circuits in Figs. 4 *A* and 6 *A* differ in phase by approximately 180 degrees, as earliest activation occurs at the top of the array for S2 at the bottom (Fig. 4 *A*) and at the bottom of the array for S2 at the top (Fig. 6 *A*). The potential gradient equals 5.4 V/cm and the preshock interval equals 172 ms (critical refractory period = 168 ms) at the critical point. In *B* and *C* earliest activation occurs distant from the S2 site, conducts around a line of block with a region of slow conduction near the S2 site, and forms a reentrant circuit, the same type of pattern seen in Fig. 4 *A*. In *B* (S2 of 150 V, S1-S2 of 197 ms) with S2 at the top and S1 at the RV side, a counterclockwise reentrant circuit is formed, the same as for Fig. 4 *A* (septal S1 with bottom S2). The two reentrant patterns, however, differ in phase by ~ 180 degrees. The potential gradient equals 5.2 V/cm and the preshock interval equals 173 ms (critical refractory period = 171 ms) at the critical point. In *C* (S2 of 150 V, S1-S2 of 197 ms), with S2 at the bottom and S1 at the RV side, a clockwise reentrant circuit is formed, the same as for Fig. 6 *A* (septal S1 with top S2). These two reentrant patterns, however, also differ in phase by ~ 180 degrees. The potential gradient equals 5.9 V/cm and the preshock interval equals 169 ms (critical refractory period = 170 ms) at the critical point.

reentry (Fig. 6 *C*). In both cases, earliest activation is again distant from the S2 site with slow conduction near the S2 site.

Thus, counterclockwise reentry is created by the combination of right S1 with bottom S2 and left S1 with top S2, the two patterns differing in phase by ~ 180 degrees due to the different sites of early activation. Conversely, clockwise reentry is created by the combination of right S1 with top S2 and left S1 with bottom S2, these two patterns also differing in phase by ~ 180 degrees. The critical points for this dog all occur at gradients of 5–6 V/cm and at preshock intervals approximately equal to the critical refractory period. The region of slow conduction occurs predominantly between the critical point and the S2 site near the presumed border of direct excitation. Even within the same animal, however, the magnitude of the area over which slow conduction occurs and the conduction velocity vary (compare Figs. 4 *A*, 6, and 7).

Change in S1-S2 interval and S2 voltage. Decreasing or increasing the S1-S2 interval moves the reentrant circuit towards or away from the S1 location, respectively. A comparison of Figs. 6 *B* and 7 *A* indicates the change in location of the reentrant circuit following a small change in the S1-S2 interval. The recovery period at the critical point in Fig. 7 *A* is 8 ms greater than that of Fig. 6 *B*, which is comparable to the 6-ms increase in the S1-S2 interval. Thus the preshock interval remains relatively constant even though the location of the critical point moves ~ 5.5 mm across the array, being 173 ms for Fig. 6 *B* and 171 ms for Fig. 7 *A*. For all dogs, increases in the S1-S2 interval moved the reentrant circuit away from the S1 site and eventually off the array, while decreases in the S1-S2 interval moved the reentrant circuit towards the S1 site and finally off the array. For both cases the changes in the S1-S2 intervals are approximately equal to the differences between the recovery periods at the original and new critical points.

For all cases in all animals, the preshock interval at the critical point is longer than the critical refractory period by 1±3 ms, indicating a close relationship between the S1-S2 interval and the recovery period at the critical point (Fig. 8). However, some variability exists as indicated by the scatter of the preshock intervals (Fig. 8). Some of this small scatter may be due to the changes in the recovery periods over time; in most dogs, the recovery periods declined by 5–15 ms over the course of the experiment. Because it was impractical to determine the recovery periods at the time of each S2 shock, all preshock intervals are compared to the refractory periods determined at the beginning of the study.

The potential gradients at the critical points also remained relatively constant, regardless of the change in the voltage of the S2 shock. Figs. 4 *A* and 7 *B* demonstrate the changes in the reentrant pattern following a decrease in the S2 voltage from 150 to 100 V. The critical point moves towards the S2 site following the decrease in the S2 voltage, but its location relative to the S1 site does not change, because the preshock intervals are almost the same. The potential gradients at the critical points are nearly identical even though the locations differ by approximately 5.5 mm; 5.8 V/cm for the 150 V S2 and 5.6 V/cm for the 100 V S2. Increases in the S2 voltage move the reentrant circuit away from the S2 site, while decreases in the S2 voltage move it toward the S2 electrode. For all reentrant circuits, the critical points occurred at sites where isogradient lines of 5.1±0.6 V/cm intersected relatively refractory tissue (Fig. 8). The mean current density at the critical point is 19.5 mA/cm^2, and the energy is 290 μJ/cm^3. Increasing the S2 voltage so that the potential gradients exceed ~ 5 V/cm over the entire array or decreasing the S2 voltage to less than ~ 5 V/cm

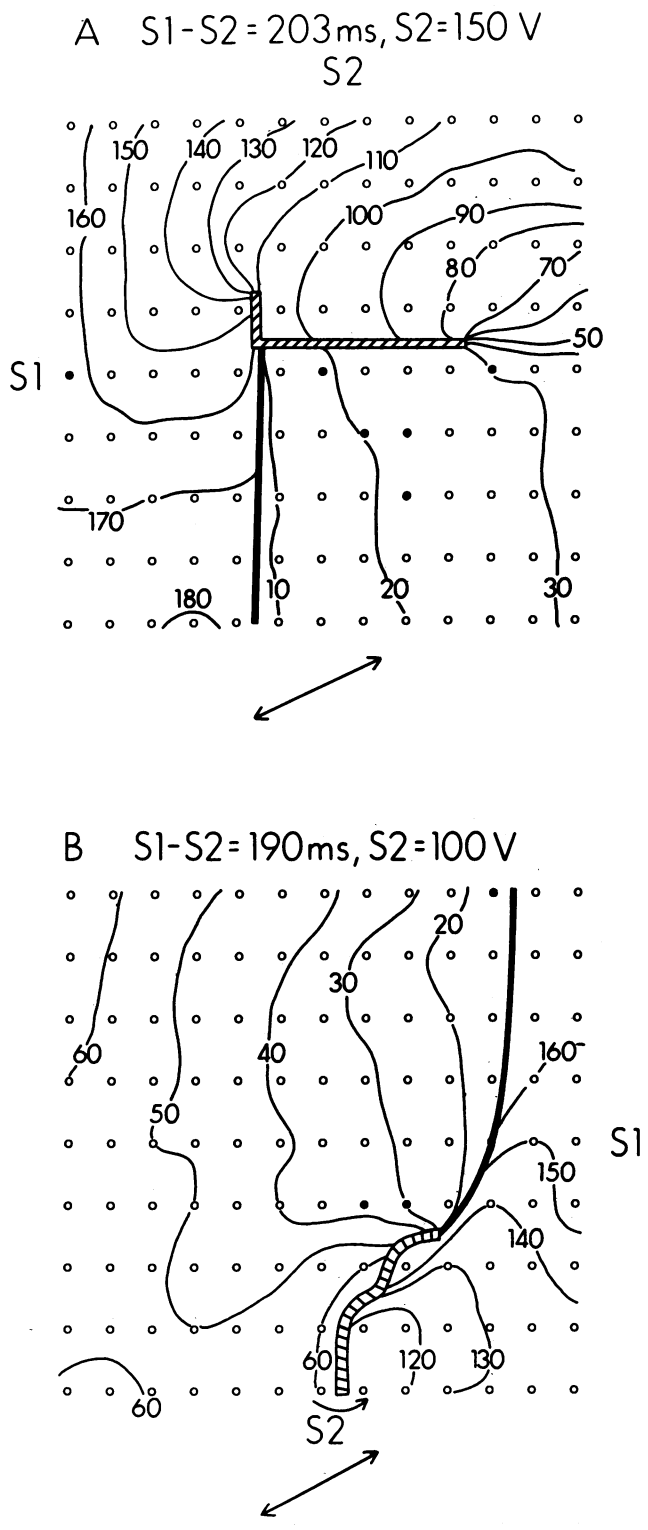

Figure 7. Effects of changing S1-S2 interval or S2 voltage on the location of the reentrant circuit. (*A*) Change in S1-S2 interval. Because the critical point occurs at a relatively constant preshock interval in each dog, increases and decreases in the S1-S2 interval moved the reentrant site away from and towards the S1 site, respectively. (*A*) The reentrant pattern following a 150 V S2 at an S1-S2 interval of 203 ms, vs. the pattern following a 150 V S2 at an S1-S2 interval of 197 ms in Fig. 6 *B*, a change in the S1-S2 interval by 6 ms. The recovery period at the critical point was 194 ms for Fig. 6 *B* and 202 ms for Fig. 7 *A*, an increase of 8 ms. Because the S1 activation patterns were nearly identical, the preshock intervals therefore differed by only 2 ms, even though the locations of the critical points differed by 5.5 mm. (*B*) Change in S2 voltage. Change in the S2 voltage produced changes in the potential gradients. Although S2 voltages of 75–175 V produced reentry within the array, the potential gradient at the critical points remained relatively constant, the mean being 5.1±0.6 V/cm. The reentrant pattern following a 100-V S2 at an S1-S2 interval of 190 ms is shown and should be compared to the pattern in Fig. 4 *A* following a 150-V S2 for identical S1 and S2 locations and almost the same S1-S2 interval (190 vs. 191 ms). Decreasing the S2 voltage moved the reentrant circuit towards the S2 site. The potential gradient at the critical point following the 100 V S2, 5.6 V/cm, remained approximately the same as that following the 150 V S2, 5.8 V/cm (Fig. 4 *A*), even though the locations of the critical points differed by 5.5 mm.

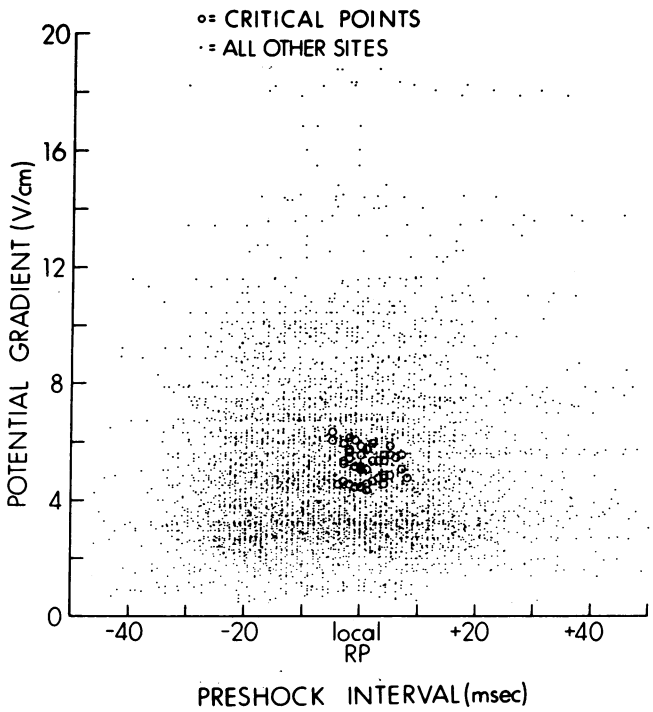

Figure 8. Preshock intervals and gradients at the critical points. The preshock intervals and the potential gradients at all critical points shown for all dogs. Although the mean refractory periods differed widely among the 11 dogs (129 to 179 ms), the preshock intervals at the critical points approximately equaled the critical refractory periods for all cases. The preshock intervals, in milliseconds, are shown on the *x*-axis referenced to the critical refractory period and the potential gradients, in V/cm, are shown on the *y*-axis. Values for critical points are shown as circles. Values for all other recording electrodes are designated as dots. For the critical points, the mean preshock interval is 1±3 ms longer than the critical refractory period, and the mean potential gradient is 5.1±0.6 V/cm.

over the entire array move the reentrant circuits off the array, away from or towards the S2 site, respectively.

A small scatter is also present in the potential gradients. Part of this scatter is probably due to errors in calculation of the gradients and to the effect of averaging the values at the four electrodes surrounding the critical point. Another possible reason for the small scatter in both potential gradients and

preshock intervals is that the critical points may occur over a range of values, i.e., a critical region. In no case, however, did reentry occur in regions of very large or small potential gradients nor did large differences occur between preshock intervals and critical refractory periods (Fig. 8).

Transmural recordings. Transmural recordings were obtained from three dogs following perpendicular interaction of isorecovery and isogradient lines. Fig. 9 shows the activation patterns following S1 pacing from the septal side and S2 stimulus from the bottom. A counterclockwise reentrant pattern is formed with earliest activation distant from the S2 site, the same pattern seen with the epicardial array (Fig. 4). Subendocardial activation occurs slightly earlier than subepicardial activation in this example, in most electrodes the difference being 4 to 6 ms. Subendocardial activation was slightly earlier in most examples, although occasionally subepicardial activation occurred earlier than midmyocardial or subendocardial activation. Slow conduction is present in two separate locations in Fig. 9 *B*, from isochrones 50–70 ms and 100 to 130 ms. The slow conduction from 100 to 130 ms occurred in a position not normally seen, possibly due to the non-parallel nature of the isorecovery lines for this dog (Fig. 9 *A*).

For all three dogs, the critical point occurs at approximately the same positions on the subendocardium as on the midmyocardium and subepicardium; thus, the locus of critical points in three dimensions is a line. The potential gradient and preshock values at the critical points and the patterns of activation are not significantly different following transmural recordings obtained with plunge needles than for the recordings obtained with the epicardial array. Thus, the plunge needles do not appear to alter significantly the patterns of activation.

Activation patterns for parallel isogradient and isorecovery lines

To understand further the patterns of activation following interactions of specific field strength and isorecovery lines, S1 pacing and S2 shocks were delivered from the same side of the epicardial array in six dogs, thus creating isorecovery and isogradient lines parallel to each other (Fig. 10, *A* and *B*). Delivery of the S2 shock at an S1-S2 interval of 198 ms produced direct excitation of most of the mapped area with activation spreading away from the directly excited border (Fig. 10 *C*). This outcome is similar to that observed in the area away from the S2 site and past the critical point for perpendicularly oriented isorecovery and isogradient lines. A decrease in the S1-S2 interval by 3 ms decreased the directly excited area with continuing spread of activation away from the directly excited border, as would be expected for stimulation of tissue slightly less recovered (Fig. 10 *D*). At the directly excited boundary, the potential gradients are < 4–6 V/cm while the recovery periods are approximately equal to the S1-S2 interval for both examples.

This pattern does not hold true following a further 3-ms decrease when the S1-S2 interval is equal to the recovery period in a region where the potential gradients are ≥ 4–6 V/cm (Fig. 10 *E*). No early activation is seen conducting away from a directly excited border; instead, earliest activation enters from outside the mapped area and spreads towards the S1 site. Slow conduction and block occur along a line approximately parallel to the S1 site, probably representing the border of direct excitation and/or graded response for this S1-S2 interval. The region proximal to the line of block (near the S1 site) is probably directly excited by the S2 stimulus because the S1-S2 interval is longer than the recovery periods for this region and the S2 field strength is strong in this region. The average potential gradients along this line of block and slow conduction are 4 to 6 V/cm. With further decrease in the S1-S2 interval, the line of slow conduction and block moves closer to the S1

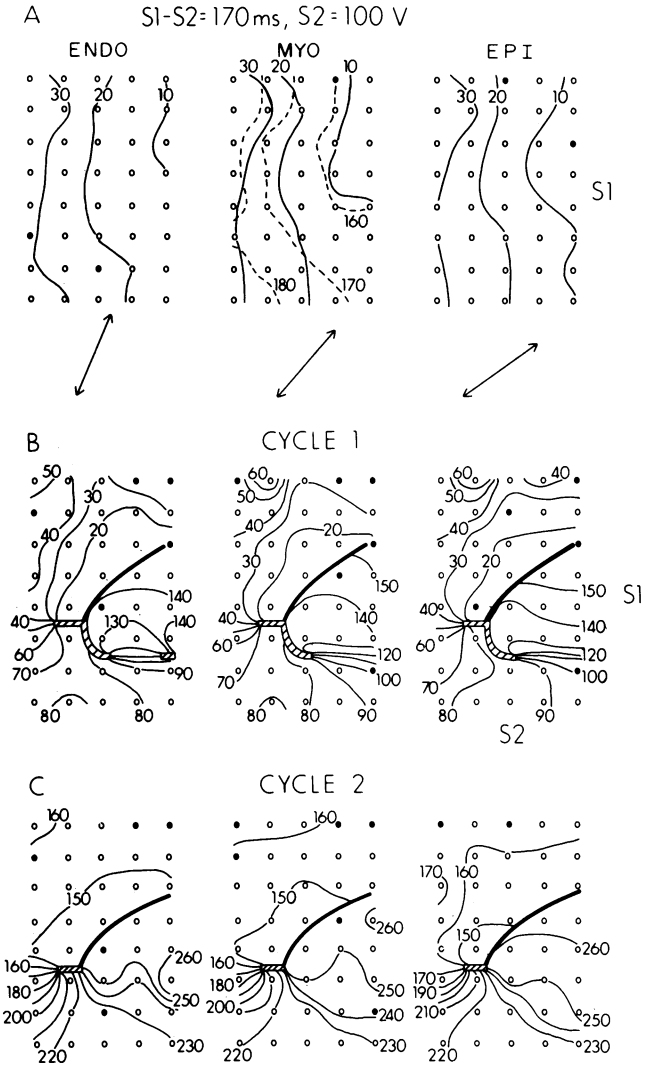

Figure 9. Transmural recordings of activation patterns following perpendicular interaction of isorecovery and isogradient lines. (*A*) The baseline S1 activation pattern (*solid lines*) with the corresponding isorecovery lines (*dashed lines*) for the midmyocardial layer. Although the S1 activation pattern is less uniform and parallel than the example in Fig. 3, the refractory periods are relatively constant within the array (149±3 ms). Only small differences are present in the transmural distribution of activation patterns. The double-headed arrow at the bottom represents the mean fiber orientation within each plane. (*B* and *C*) The first and second cycles of reentry, respectively, following a 100-V S2 at an S1-S2 interval of 170 ms. A counterclockwise reentrant pattern is created with earliest activation distant from the S2 site, similar to the epicardial pattern seen in Fig. 4 *A*. The line of block and the critical point occur along the 170 ms recovery period isochrone, the same value as the S1-S2 interval at which the S2 shock was delivered. The potential gradient equals 5.7 V/cm and the preshock interval equals 148 ms (critical refractory period = 148 ms) at the critical point.

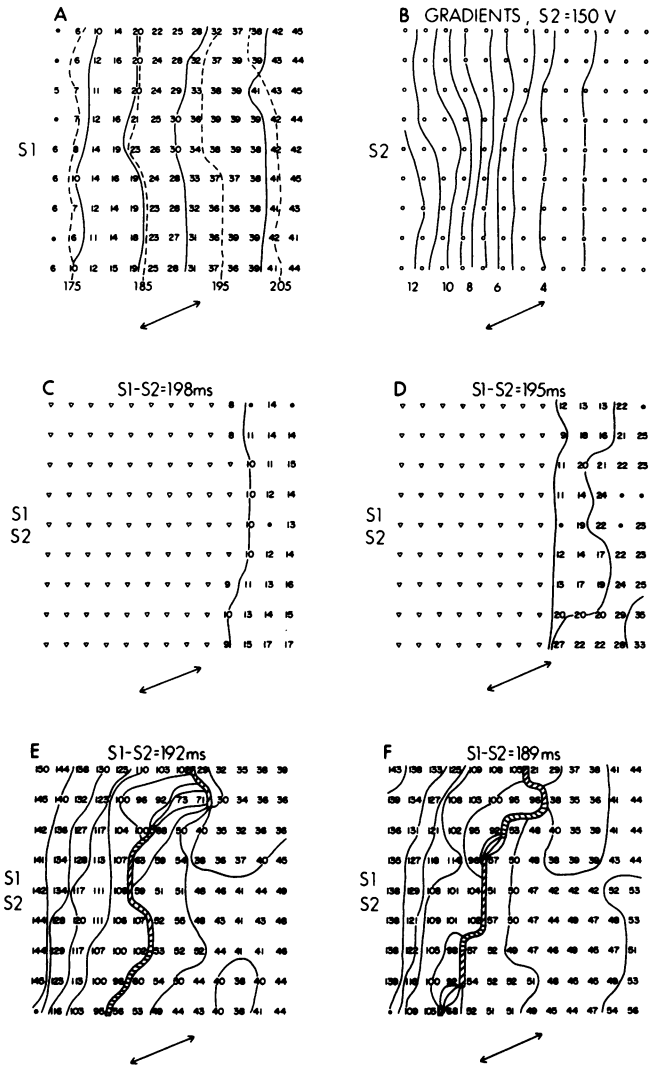

Figure 10. Activation patterns for parallel isorefractory and isogradient lines. (*A*) The S1 activation pattern and recovery periods following S1 pacing from the left. The isochronal and isorecovery lines are nearly parallel ($r = 0.94$). The double-headed arrows in *A* and *B* represent the mean epicardial fiber orientation under the array. (*B*) The distribution of potential gradients for a 150 V S2 from the left. Gradients of 4–6 V/cm occur at the center of the array. (*C* and *D*) The initial activation patterns following S2 shocks of 150 V at S1-S2 intervals of 198 and 195 ms, respectively. In both cases early activation conducts away from the presumed border of direct excitation. The triangles represent areas thought to be directly excited by the S2 shock. A decrease in the S1-S2 interval moves the directly excited border closer to the S1 site (*D*). The double-headed arrows represent the mean epicardial fiber orientation along the border of direct excitation in *C* and *D* and the mean epicardial fiber orientation along the region of conduction block in *E* and *F*. (*E*) The initial activation pattern following a further decrease in the S1-S2 interval to 192 ms. Early activation no longer conducts away from the boundary of a directly excited region; instead, activation enters from outside the array and conducts towards the S1 site. The wave of activation encounters a line of block or slow conduction, shown by the hatched line. This region of slow conduction and block may represent the border of the directly excited region, with activation blocking or conducting slowly because the tissue is refractory following direct excitation by the S2 field. The directly excited region is not indicated by triangles in order to demonstrate the patterns of activation across the region; however, this area is assumed to be directly excited by the S2 shock. The potential gradients along this line of block and slow conduction are 4 to 8 V/cm. A further 3-ms decrease in the S1-S2 interval to 189-ms (*F*) moves this border slightly closer to the S1 site, directly exciting less tissue.

site, indicating progressive decrease in size of the directly excited region (Fig. 10 *F*). Thus, absence of conduction away from the border of direct excitation occurs at specific interactions of stimulus strength and tissue refractoriness, the same situation occurring for perpendicularly oriented isorecovery and isogradient lines.

Parallel isorecovery and isogradient lines were not always created by S1 and S2 stimulation on the same side of the array. Nonparallel S1 activation patterns, usually due to rapid endocardial conduction, resulted in the creation of isorecovery and isogradient line intersections at various angles between 0 and 90 degrees. In these instances, reentry occurred within the mapped area, similar to the patterns following perpendicular interactions. Early activation typically occurred along one portion of an isogradient line with lack of conduction away from the other portion. Decrease in the S1-S2 interval, however, eventually lead to absence of conduction away from the directed excited region across the entire width of the array, as for parallel oriented isorecovery and isogradient lines.

Effects of fiber orientation on activation patterns

The orientations of the lines of block and the long axis of the myocardial fibers were measured relative to the horizontal axis of the mapped area for both the epicardial and transmural recordings. The orientations of the lines of block around which the reentrant circuits develop did not correlate with the local fiber orientations ($r = 0.18$), the mean difference in these orientations being 43 degrees. Within individual dogs the orientation of the line of block varied widely for different reentrant cycles depending on the location of the S1 and S2 sites and the pattern of recovery of refractoriness before the S2 shock (Figs. 4, 6, 7).

In many reentrant circuits, sharply curved lines of block exist (Figs. 6, *B* and *C*). For such examples in which the lines of block spanned more than one pair of recording electrodes, the orientations of the different sections of the line of block were individually compared to the fiber orientation. For example, in Fig. 6 *B* the line of block has segments at 0 and 90 degrees, compared to the local fiber orientation of 29 degrees. For most transmural recordings, the orientations of the lines of block are nearly identical throughout the myocardium (Fig. 9). Because the fibers rotate between the different planes of tissue, the area of block occurs at different orientations of fiber direction depending on the plane of tissue.

The choice of 0.1 m/s as a lower limit for conduction velocity to identify conduction block may not be correct. The activation maps were usually consistent with this choice, however, with isochronal lines approaching or travelling at right angles to the lines of block rather than emanating away from them as would be expected if slow conduction, and not block, were present. If the lower limit of conduction velocity is made smaller, the conclusions of the study still hold, although some of the quantitative values change. For example, use of a lower limit of conduction velocity of 0.05 m/s results in conduction block only between the two electrode sites with activation times of 68 and 137 ms in Fig. 4 *A*. If a lower limit of conduc-

tion velocity of 0.02–0.03 m/s is used, most reentrant circuits appear to rotate around very short regions of block, most < 2–3 mm diam (Table I). The use of 0.05 m/s or slower conduction velocities did not increase the relationship between fiber orientation and the lines of block.

Slow conduction did not appear to occur predominantly along or across the fibers. Rather, slow conduction appeared to be associated with the location of the S2 site and the approximate border of direct excitation. For example, in Fig. 6, *B* and *C*, slow conduction occurs both across and along the approximate long axis of the local fiber orientation, respectively.

Discussion

Nonuniform dispersion of recovery and reentry

The induction of reentry depends on the creation of a region of temporary or permanent unidirectional conduction block (34). Nonuniform dispersion of recovery has been assumed to be the mechanism creating this region of temporary unidirectional block (1–5). According to this hypothesis, a premature stimulus produces activation fronts that conduct away from the stimulus site and then block in regions of greater refractoriness. Reentry occurs if tissue proximal to the region of block has recovered by the time activation fronts arrive from the distal portion of the region of block. This theory is supported by numerous studies demonstrating lower fibrillation thresholds as the dispersion of refractoriness is increased (1, 2, 10, 11, 14), and by studies showing the formation of reentry around lines of block created in regions containing disparities of refractoriness (35).

To initiate reentry according to this hypothesis, large differences in the degree of recovery must exist prior to the application of the inducing stimulus. Otherwise, premature stimulation should merely result in the propagation of wavefronts away from the site of earliest capture following S2 stimulation, as no abrupt change in refractoriness exists to produce unidirectional block. It is known, however, that reentry can be induced in myocardium that possesses small inherent differences in refractoriness (~ 10–20 ms) (5, 6, 35–37).

In this study, uniform parallel isorecovery lines were created following S1 stimulation that highly correlate ($r = 0.95 \pm 0.03$) with the uniform S1 activation isochrones for all dogs (Figs. 3, 9 *A*, 10 *A*). The range of the standard deviations of the refractory periods for all dogs is 1–4 ms, indicating that significant nonuniform dispersion of refractoriness did not exist immediately before the S2 stimulus. In addition, the reentrant sites and regions of conduction block do not occur at the same location within individual dogs as would be expected if a region of nonuniform dispersion of refractoriness were the primary determinant for the induction of reentry. Rather, the sites of reentry and block change position as the S1 and S2 locations, S1-S2 interval, and S2 strength are altered (Figs. 4, 6, 7). These findings correlate with those of Chen et al. (6) who demonstrated the induction of figure-of-eight reentry in normal myocardium devoid of large changes in refractoriness, and imply that other mechanisms are more important than the nonuniform dispersion of recovery in the induction of reentry by suprathreshold electrical stimuli. These findings do not negate the possible importance of the nonuniform dispersion of recovery in the induction of reentry by other means or in the degeneration of electrically induced reentrant circuits into fibrillation.

Table I. Conduction Velocity and Length of Block

Conduction velocity	Length of block	Number without block
m/s	*mm*	
0.1	11.1±4.9	0
0.05	5.6±2.4	5
0.03	0.9±1.6	34
0.01	0	55

The conduction velocity is the minimum velocity allowed below which conduction block occurs. The length of block is the mean value from all episodes of reentry in all dogs following orthogonal interaction of isorefractory and isogradient lines. Number without block refers to episodes of reentry in which conduction block could not be detected between any recording electrodes for the indicated lower limit velocity. In these cases a conduction block length of 0 mm was assigned. No sites of block could be detected for the conduction velocity 0.01 m/s.

Fiber orientation and reentry

Recently, the importance of fiber orientation has been emphasized for the induction and maintenance of reentrant circuits (12, 18, 19). Spach et al. (18) demonstrated a reduced safety factor for conduction along versus across the fiber axis following premature stimulation which can create a region of temporary unidirectional conduction block leading to reentry in the absence of large inherent differences in refractoriness. Other investigators have demonstrated ellipsoidal reentrant circuits with the long axis of the circuits parallel to the long axis of the myocardial fibers (12, 19). These recent studies, however, fail to explain why single premature stimulation at low currents rarely induces fibrillation in normal myocardium. Rather, stimulus currents of at least 10–20 mA are usually required for a single S2 stimulus to induce reentry (9, 11, 13–17).

Although fiber orientation may be important in the initiation or maintenance of reentry in other situations, it appears to play a minimal role in the induction of reentry by the suprathreshold electrical stimuli used in this study. The orientations of the lines of block around which the reentrant circuits develop do not correlate with the local fiber orientation ($r = 0.18$). Transmural recordings also fail to show a strong influence of fiber orientation on the location of block (Fig. 9), since the transmural rotation of fibers from epicardium to endocardium does not yield a similar rotation in the line of block. The results obtained with parallel isorecovery and isogradient lines also imply that the line of block and area of slow conduction are determined not by fiber orientation, but primarily by the border of direct excitation (Figs. 10, *E* and *F*).

Critical points and reentry

Mechanism for the initiation of reentry and creation of a critical point. Because neither nonuniform dispersion of recovery nor fiber orientation appears critical for the induction of reentry by suprathreshold electrical stimuli, an alternative mechanism is needed. Two recent studies report that activation following a premature suprathreshold stimulus begins distant from the S2 stimulation site (6, 22). Although S2 field strengths were not measured in either study, both propose that unidirectional block at the border of direct excitation in re-

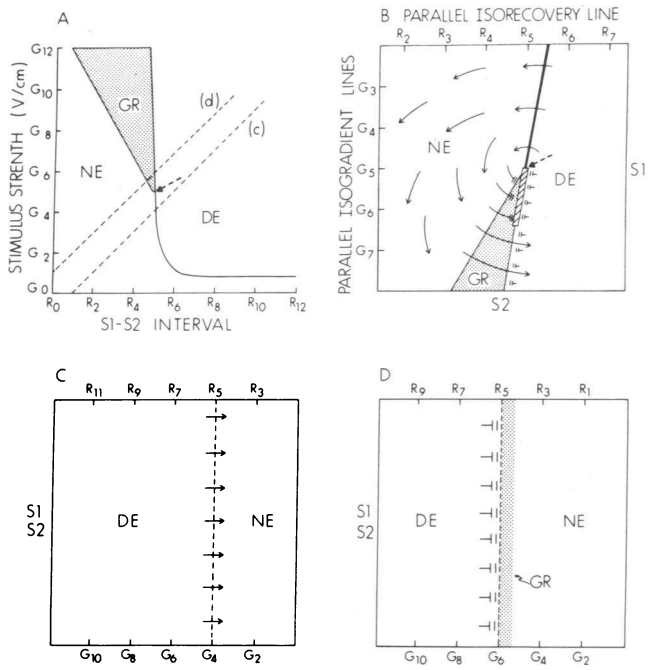

Figure 11. Graded response theory for reentry. (*A*) Strength interval curve. A modified strength-interval curve is shown, with stimulus strength in volts per centimeter on the *y*-axis and S1-S2 interval, or refractoriness, on the *x*-axis. On the *y*-axis, G_{12} represents the largest potential gradient and G_0 the smallest. On the *x*-axis, R_{12} represents the most recovered tissue and R_0 the most refractory. R_0 does not represent phase 0 of the action potential, but merely tissue fully refractory to a premature stimulus. Interaction of the isorecovery and isogradient lines produces either direct excitation (DE), graded response (GR), or neither effect (NE). The potential gradient at G_5 is ~ 5 V/cm while the potential gradient at the rheobase is ~ 0.8 V/cm (24). The critical refractory period (for the 2 mA stimuli) equals the preshock interval at R_5. The dashed arrow represents the position of the critical point in this panel and in *B*. The dashed lines labeled "c" and "d" are described in *C* and *D*. (*B*) Perpendicular isorecovery and isogradient lines. A diagramatic representation of the results of Fig. 4 *A* is shown, with gradient and refractory values corresponding to the diagram in *A*. The row of pacing wires (S1) on the right creates parallel isorecovery lines (R_7 through R_2), with R_7 the least refractory and R_2 the most refractory. The S2 from the bottom creates parallel isogradient lines (G_7 through G_3), with G_7 the largest gradient and G_3 the weakest. The solid and hatched lines are the frame and block lines, respectively. The ⊣| represent areas of temporary unidirectional conduction block. For this idealized diagram, the S1-S2 interval equals the recovery period (preshock interval equals the critical refractory period) at R_5, and the S2 voltage creates a potential gradient of 5 V/cm at G_5. The S2 shock directly excites the area near the S1 site (*DE*) and produces a region of graded response (*GR*). Activation fronts only propagate away from part of the directly excited area, activation fronts do not propagate away from the directly excited area abutting regions of graded response, thus forming an area of temporary unidirectional conduction block. An activation front conducting towards the S2 site from the early sites of activation produces another region of conduction block (*hatched line*) when it enters tissue insufficiently repolarized from graded response or direct excitation. When the myocardium has recovered, activation can conduct through this area and form a reentrant circuit, as shown by the arrows spanning the GR zone and entering the DE zone. (*C* and *D*) Parallel isorecovery and isogradient lines. S1 pacing and the S2 shock are delivered from the same side of the array, as in Fig. 10. In *C*, the S2 shock creates a potential gradient of ~ 5 V/cm at G_5, and is delivered at an S1-S2 interval such that R_5 intersects G_4, thus forming a directly excited boundary from which activation conducts away. No region of graded response is formed by this interaction of isorecovery and isogradient lines (*dashed line* "c", *A*), creating the same situation as in Figs. 10, *C* and *D*. Decreasing the S1-S2 interval, however, yields isorecovery-isogradient interactions that produce a region of graded response (*dashed line* "d" in *A*), and thus temporary unidirectional block, distal to the directly excited area (*D*), similar to the experimental data in Fig. 10, *E* and *F*. Activation fronts cannot enter the directly excited area until the tissue has repolarized, thus slow conduction and/or block occurs along the nearly vertical directly excited border when wavefronts conduct inward from tissue not directly excited by the S2 shock, again similar to the patterns seen in Fig. 10, *E* and *F*.

gions of high S2 field strength may be the mechanism underlying the formation of reentrant circuits.

The present study was designed to determine if a critical point exists around which reentry develops, and, if so, the strength and timing of the stimuli that cause this critical point. This was accomplished by creating parallel uniform isorecovery and isogradient lines oriented perpendicular to each other (Figs. 2 and 3), which allowed identification of the critical isogradient and critical isorecovery lines, i.e., the lines at whose intersection the critical point exists.

Activation fronts after the S2 shock conduct away from the directly excited region towards tissue exhibiting greater refractoriness (longer recovery periods). Poststimulus conduction is rapid away from the directly excited region where the stimulus field is weakest but is somewhat slower where the stimulus field is slightly larger. This slower conduction can probably be explained by the fact that the stronger stimulus field directly excites tissue that is more refractory, so that poststimulus conduction occurs in less recovered myocardium. Where the potential gradient field created by the S2 stimulus is more than ~ 5 V/cm, activation does not conduct away from the boundary of the region of direct excitation. Thus, earliest poststimulus activation occurs only distant from the S2 site. The absence of conduction away from the directly excited region in areas of high gradient can be thought of as a type of temporary unidirectional conduction block.

The mechanism for the unidirectional block induced by the S2 stimulus is unknown. One possible mechanism is the induction of a graded response, which causes a temporary prolongation of refractoriness. A graded response and prolongation of refractoriness occur during stimulation of relatively refractory tissue, with the magnitude and resulting prolongation of refractoriness dependent on both the strength and timing of stimulation (38). While the exact extent of the region of graded response on the strength-interval plot is not definitely known, we hypothesize its location to be that shown by the stippled area in Fig. 11 *A*. In Fig. 11 *B*, unidirectional block away from the directly excited area occurs where the graded response is assumed to be present, creating an activation front that terminates at the critical point. The portion of the activation front near this blind end rotates towards the S2 electrode to conduct into the tissue adjacent to the region of graded response. If the tissue is sufficiently recovered, activation then conducts through the regions of graded response and direct excitation and forms circus reentry. Thus, the stimulus itself induces temporary inhomogeneity of refractoriness and unidi-

rectional conduction block that can lead to reentry. These ideas are speculative and await experimental evaluation.

The creation of an activation front that blindly terminates may not by itself produce a reentrant circuit. Another prerequisite may be the recovery of the directly excited tissue (and the tissue undergoing graded response, if it exists) before the arrival of the activation fronts swinging around from the other side of the critical point. Otherwise, bidirectional conduction block would occur and abort the reentrant circuit. This concept explains the mechanism for the formation of the conduction block lines around which the activation front rotates. The early activation fronts conduct rapidly away from the border of the directly excited area into tissue that was not directly excited by the S2 field. As fronts conduct downward towards the S2 site, they encounter tissue with prolonged refractoriness due to direct excitation and possibly graded response. Because the tissue initially is not recovered at the time of arrival of activation fronts, a short region of block is created (*hatched line,* Fig. 11 *B*). The length of this block depends on the rapidity with which early activation fronts reach this region after conducting away from the directly excited boundary on the opposite side of the critical point and also depends on the time course of recovery of the tissue. Factors that increase the length of this block line, such as prolonged refractoriness or rapid conduction, would decrease the probability that a reentrant circuit would form (39). Because activation fronts conduct into relatively refractory tissue in this region, conduction velocity is slow (Figs. 4, 6, 7, 9, 10). In most cases activation fronts entered the directly excited area after a shorter time interval than the refractory period following S1 stimulation (Fig. 4 *A*). The results are consistent with the finding that action potential duration is shortened by premature stimulation (2). Thus, the reentrant circuit may rotate around a line of block, the length of which is not precisely known since the estimated length varies with the assumed value of the slowest possible conduction velocity (Table I).

Movement of the S1 site to the opposite side of the array changes the reentrant circuit from clockwise to counterclockwise because the right-left orientation of the directly excited region to the region excited by conduction is reversed (compare to Figs. 6, *A* to *B,* Figs. *C* to 4 *A*). The phase of the latencies, i.e., the location of earliest activation near the critical point, is changed only slightly, because the up-down orientation of the two regions remains approximately the same, since the S2 site remains constant. Because initial unidirectional block occurs near and early activation occurs far from the S2 site, movement of the S2 location reverses the orientation of these two regions. Therefore, movement of the S2 site alters the orientation of reentry from clockwise to counterclockwise and changes the site of earliest activation, thereby altering the phase by approximately 180 degrees (Figs. 6 *A* to 4 *A,* Figs. 6 *C* to *B*).

The critical points occurred over narrow ranges: preshock intervals being 1±3 ms longer than the critical refractory periods and potential gradients being 5.1±0.6 V/cm (Fig. 8). The majority of the scatter occurred among various animals, not among different episodes of reentry in the same animal. Other factors in addition to differences from animal to animal may also have contributed to this scatter, such as (*a*) a 5- to 15-ms decline in the refractory periods over time, (*b*) errors in calculation of the potential gradients, and (*c*) the possibility that the critical points may occur over a range of values, i.e., a critical region instead of a critical point. The potential gradient magnitude for excitation of fully repolarized myocardium is dependent on the local fiber orientation (29); thus, the critical point may also depend on the fiber orientation relative to the isogradient lines. The values of preshock interval and potential gradient at the critical point may be influenced by the particular stimulus waveform and duration used.

Length of conduction block, point stimulation, and parallel isogradient and isorefractory lines. The length of the region of temporary unidirectional conduction block required for the electrical induction of reentry is uncertain from our data, although a mean length of ~ 11 mm would be necessary if identification of conduction block is based on 0.1 m/s as the lower limit of conduction velocity. If even slower conduction can occur in normal ventricular muscle (0.01–0.05 m/s) as reported for atrial muscle (40) and for abnormal ventricular muscle (19), very short regions of initial block (1–2 mm) could create the conditions necessary to initiate and sustain reentry. Based on experimental data (29), modeling studies indicate that point stimulation with 10 mA produces a potential gradient magnitude of 5 V/cm approximately 2 mm from the point source (Frazier and Krassowska, unpublished observation). Thus, with a lower limit of conduction velocity of 0.03 m/s or less, the distance between the stimulus site and critical point is greater than the length of conduction block observed in this study (Table I). Thus, a reentrant circuit can be maintained. Stimulus currents of only a few milliamperes, however, would not produce sufficiently large potential gradients to induce a great enough region of graded response and temporary block to support the initiation of a reentrant circuit, i.e., the critical point would not be created or would be located too close to the S2 stimulation site to support reentry. This could explain why stimulus currents greater than 10 mA are usually necessary for the electrical induction of fibrillation using single premature stimuli in normal canine and human ventricles (9, 11, 13–17).

Isorecovery and isogradient lines do not have to be precisely perpendicular for the induction of reentry. Any angle of interaction other than parallel can create critical points. For example, interaction of an elliptical or circular potential gradient field produced by point stimulation (29) with a linear dispersion of refractoriness will yield twin critical points and mirror image circus patterns of reentry (6, 20). This would be analogous to extending the plane of S1 stimulation in Fig. 11 *B* below the S2 site, thus forming mirror image reentrant circuits above and below the S2 site, similar to superimposing the S2 electrodes of Figs. 4 *A* and 6 *A*. Chen et al. (6) obtained similar qualitative results using S1 and S2 point stimulation 1 to 2 cm apart on the endocardial surface of the canine right ventricle. In that study, figure-of-eight reentry occurred following S2 stimulation of 10–100 mA, and the earliest poststimulus activation occurred distant from the S2 site, between the S1 and S2 locations, as would be predicted based on the existence of critical points.

The only apparent interaction of isorecovery and isogradient lines unable to create a critical point and reentry is a parallel orientation. This type of orientation is shown experimentally in Fig. 10 and diagrammatically in Fig. 11 *C* and *D*. No critical point is created because either early activation conducts away from the entire border of direct excitation (Figs. 10, *C* and *D,* 11 *C*) or lack of conduction occurs along the entire border (Figs. 10, *E* and *F,* 11 *D*).

This model does not necessarily apply to situations in which tissue abnormalities are present. Factors producing ischemia, anatomic abnormalities, depressed conduction, or large disparities in repolarization can create regions of unidirectional block and thus support the induction of reentry independent of the isorecovery-isogradient interactions. In these cases, inhomogeneity is present before the application of the premature stimulus; thus, stimulus-induced inhomogeneity is not a necessary prerequisite for the induction of reentry. Also, the interaction of a uniformly changing potential gradient field with a region of nonuniform dispersion of recovery could create several critical points which might be more arrhythmogenic than the single critical point observed in the experimental model of this study. Although fiber orientation does not appear to be important in the initiation of reentry in this study, it may play a role we were unable to detect in the conduction velocity characteristics of the reentrant circuits.

Correlation to theory. Based on the phase resetting patterns of various periodic oscillators such as cardiac pacemakers (20, 21, 41–44), Winfree has developed a topological model demonstrating the unavoidable existence of a critical point which he calls a "phase singularity." At a phase singularity, the interaction of a specific stimulus within the natural cycle of the oscillator causes the response of the oscillator to become undefined. Winfree has applied these concepts to cardiac muscle and predicted the clockwise reentrant conduction patterns for the S1-S2 configuration shown in Fig. 6, *A* and *C* and counterclockwise patterns for the S1-S2 configuration shown in Figs. 4 and 6 *B* (20).

All systems of rotating waves studied by Winfree require a certain minimum region around which the phases or excitable fronts rotate, and which may correspond to the region of conduction block in our study. Because of our wide electrode spacing and inability to record transmembrane potentials, the characteristics of conduction and block in the center of the reentrant circuit could not be precisely determined. Instead of a discrete line of block, a region of abnormal conduction and block may have been present at the center of the reentrant circuit. Allessie et al. (45) have postulated that the center of the vortex in leading circle reentry is continuously invaded by multiple centripetal wavefronts which are blocked in the center of the circuit when they encounter refractory tissue. The converging wavefronts and region of central block thus form a functional obstacle around which the leading circle rotates. Based on this explanation, the minimum region for cardiac muscle would depend on electrophysiologic properties such as conduction velocity, the time of recovery of excitability, and the stimulating efficacy of the advancing wavefront.

Regardless of the precise size and mechanism of events within the central region, this study indicates that the dispersion of stimulus strength is equally as important as the dispersion of recovery in the creation of reentry by suprathreshold electrical stimulation. This finding may have application to the upper limit of vulnerability and electrical defibrillation (46).

Acknowledgments

We wish to thank Dr. Joseph C. Greenfield, Jr. for his support, Ms. Sharon D. Bowling, Ms. Ellen G. Dixon, Mr. Ned D. Danieley, and Mr. Dennis L. Rollins for their technical assistance, Ms. Cloyce M. Lassiter for her secretarial assistance, and Ms. Betty Goodfellow for preparation of the tissue sections.

Supported in part by the National Institutes of Health research grants HL-28429, HL-33637, and HL-17670, the National Science Foundation Engineering Research Center Agreement No. CDR-8622201, and by CPI Inc. and Physio-Control Corp. Dr. Frazier was supported in part by an American Heart Association Medical Student Research Scholarship. Dr. Tang is the recipient of a Canadian Heart Foundation Fellowship.

References

1. Surawicz, B. 1984. Ventricular fibrillation II: Progress report since 1971. *Clin. Prog. Pacing and Electrophysiol.* 2:395–419.

2. Han, J., and G. K. Moe. 1964. Nonuniform recovery of excitability in ventricular muscle. *Circ. Res.* 14:44–60.

3. Han, J., and B. G. Goel. 1972. Electrophysiologic precursors of ventricular tachyarrhythmias. *Arch. Intern. Med.* 129:749–755.

4. Kuo, C. S., K. Munakata, C. P. Reddy, and B. Surawicz. 1983. Characteristics and possible mechanism of ventricular arrhythmia dependent on the dispersion of action potential durations. *Circulation.* 67:1356–1367.

5. Allessie, M. A., F. I. M. Bonke, and F. J. G. Schopman. 1976. Circus movement in rabbit atrial muscle as a mechanism of tachycardia. II. The role of nonuniform recovery of excitability in the occurrence of unidirectional block, as studied with multiple microelectrodes. *Circ. Res.* 39:168–177.

6. Chen, P-S., P. D. Wolf, E. G. Dixon, N. D. Danieley, D. W. Frazier, W. M. Smith, and R. E. Ideker. 1988. Mechanism of ventricular vulnerability to single premature stimuli in open chest dogs. *Circ. Res.* 62:1191–1209.

7. Merx, W., M. S. Yoon, and J. Han. 1977. The role of local disparity in conduction and recovery time on ventricular vulnerability to fibrillation. *Am. Heart J.* 94:603–610.

8. Moore, E. N., J. F. Spear, and L. N. Horowitz. 1973. Effect of current pulses delivered during the ventricular vulnerable period upon the ventricular threshold. *Am. J. Cardiol.* 32:814–822.

9. Han, J., P. G. deJalon, and G. K. Moe. 1964. Adrenergic effects on ventricular vulnerability. *Circ. Res.* 14:516–524.

10. Han, J., P. G. deJalon, and G. K. Moe. 1966. Fibrillation threshold of premature ventricular responses. *Circ. Res.* 18:18–25.

11. Hoffman, B. F., A. A. Siebens, P. F. Cranefield, and C. M. Brooks. 1955. The effect of epinephrine and norepinephrine on ventricular vulnerability. *Circ. Res.* 3:140–146.

12. Schalij, M. J., M. A. Allessie, W. J. Lammers, and F. V. Kaam. 1987. Reentry in anisotropic ventricular myocardium. *Circulation.* 76:IV–113. (Abstr.)

13. Anderson, J. L., H. E. Rodier, and L. S. Green. 1983. Comparative effects of beta-adrenergic blocking drugs on experimental ventricular fibrillation threshold. *Am. J. Cardiol.* 51:1196–1202.

14. Moore, E. N., and J. F. Spear. 1975. Ventricular fibrillation threshold. *Arch. Intern. Med.* 135:446–453.

15. Hoffman, B. F., E. F. Gorin, F. S. Wax, A. A. Siebens, and C. M. Brooks. 1951. Vulnerability to fibrillation and the ventricular-excitability curve. *Am. J. Physiol.* 167:88–94.

16. Hoffman, B. F., E. E. Suckling, and C. M. Brooks. 1955. Vulnerability of the dog ventricle and effects of defibrillation. *Circ. Res.* 3:147–151.

17. Kowey, P. R., S. Khuri, M. Josa, R. L. Verrier, S. Sharma, J. P. Kiely, E. D. Folland, and A. F. Parisi. 1984. Vulnerability to ventricular fibrillation in patients with clinically manifest ventricular tachycardia. *Am. Heart J.* 108:884–889.

18. Spach, M. S., W. T. Miller, III, D. B. Geselowitz, R. C. Barr, J. M. Kootsey, and E. A. Johnson. 1981. The discontinuous nature of propagation in normal canine cardiac muscle. Evidence for recurrent discontinuities of intracellular resistance that affect the membrane currents. *Circ. Res.* 48:39–54.

19. Dillon, S. M., M. A. Allessie, P. C. Ursell, and A. L. Wit. 1988. Influences of anisotripic tissue structure on reentrant circuits in the epicardial border zone of subacute canine infarcts. *Circ. Res.* 63:182–206.

20. Winfree, A. T. 1987. When time breaks down: The three-dimensional dynamics of electrochemical waves and cardiac arrhythmias. Princeton University Press, Princeton, NJ. 153.

21. Winfree, A. T. 1983. Sudden cardiac death. *Sci. Am.* 248:144–161.

22. Shibata, N., P-S. Chen, E. G. Dixon, P. D. Wolf, N. D. Danieley, W. M. Smith, and R. E. Ideker. 1988. Influence of shock strength and timing on induction of ventricular arrhythmias in dogs. *Am. J. Physiol.* 255:H891–H901.

23. Amlie, J. P., and T. Owren. 1979. The effect of prolonged pentobarbital anaesthesia on cardiac electrophysiology and inotropy of the dog heart in situ. *Acta Pharmacol. Toxicol.* 44:264–271.

24. Frazier, D. W., W. Krassowska, P-S. Chen, P. D. Wolf, N. D. Danieley, W. M. Smith, and R. E. Ideker. 1988. Transmural activations and stimulus potentials in three-dimensional anisotropic canine myocardium. *Circ. Res.* 63:135–146.

25. Gaum, W. E., V. Elharrar, P. D. Walker, and D. P. Zipes. 1977. Influence of excitability on the ventricular fibrillation threshold in dogs. *Am. J. Cardiol.* 40:929–939.

26. Smith, W. M., A. L. Funk, R. E. Ideker, F. R. Bartram, and P. V. Talbert. 1982. A microcomputer-based multichannel data acquisition system for the study of complex arrhythmias. *Proc. Computers Cardiol.* 131–134.

27. Wolf, P. D., J. M. Wharton, C. D. Wilkinson, W. M. Smith, and R. E. Ideker. 1986. A method of measuring cardiac defibrillation potentials. Proc. 39th Annual Conf. on Engineering in Medicine and Biology. 4.

28. Wolf, P. D., N. D. Danieley, R. E. Ideker, and W. M. Smith. 1985. A digital tape recorder for electrophysiologic waveforms. Proc. 38th Annual Conf. on Engineering in Medicine and Biology. 124.

29. Frazier, D. W., W. Krassowska, P-S. Chen, P. D. Wolf, E. G. Dixon, W. M. Smith, and R. E. Ideker. 1988. Extracellular field required for excitation in three-dimensional anisotropic canine myocardium. *Circ. Res.* 63:147–164.

30. Funada, T., T. Iwase, and T. Iwa. 1983. Method for computerised display of epicardial maps. *Med. Biol. Eng. Comp.* 21:418–423.

31. Bartram, F. R., R. E. Ideker, and W. M. Smith. 1981. A system for the parametric description of the ventricular surface of the heart. *Comput. Biomed. Res.* 14:533–541.

32. Perlman, G. 1980. Data analysis programs for the UNIX operating system. *Behavior Research Methods Instrument.* 12:554–558.

33. Lepeschkin, E., J. L. Jones, S. Rush, and R. E. Jones. 1978. Local potential gradients as a unifying measure for thresholds of stimulation, standstill, tachyarrhythmia and fibrillation appearing after strong capacitor discharges. *Adv. Cardiol.* 21:268–278.

34. Mines, G. R. 1914. On circulating excitations in heart muscles and their possible relation to tachycardia and fibrillation. *Trans. Roy. Soc. Can.* 4:43–52.

35. Gough, W. B., R. Mehra, M. Restivo, R. H. Zeiler, and N. El-Sherif. 1985. Reentrant ventricular arrhythmias in the late myocardial infarction period in the dog. 13. Correlation of activation and refractory maps. *Circ. Res.* 57:432–442.

36. Moe, G. K., A. S. Harris, and C. J. Wiggers. 1941. Analysis of the initiation of fiberillation by electrographic studies. *Am. J. Physiol.* 134:473–492.

37. van Capelle, F. J. L., and D. Durrer. 1980. Computer simulation of arrhythmias in a network of coupled excitable elements. *Circ. Res.* 47:454–466.

38. Kao, C. Y., and B. F. Hoffman. 1958. Graded and decremental response in heart muscle fibers. *Am. J. Physiol.* 194:187–196.

39. Rensma, P. L., M. A. Allessie, W. J. E. P. Lammers, F. I. M. Bonke, and M. J. Schalij. 1988. Length of excitation wave and susceptibility to reentrant atrial arrhythmias in normal conscious dogs. *Circ. Res.* 62:395–410.

40. Spach, M. S., P. C. Dolber, and J. F. Heidlage. 1988. Influence of the passive anisotropic properties on directional differences in propagation following modification of the sodium conductance in human atrial muscle a model of reentry based on anisotropic discontinuous propagation. *Circ. Res.* 62:811–832.

41. Winfree, A. T. 1975. Unclocklike behavior of biological clocks. *Nature (Lond.).* 253:315–319.

42. Jalife, J., V. A. J. Slenter, J. J. Salata, and D. C. Michaels. 1983. Dynamic vagal control of pacemaker activity in the mammalian sinoatrial node. *Circ. Res.* 52:642–656.

43. Jalife, J., and C. Antzelevitch. 1979. Phase resetting and annihilation of pacemaker activity in cardiac tissue. *Science (Wash. DC).* 206:696–697.

44. Antzelevitch, C., and G. K. Moe. 1983. Electrotonic inhibition and summation of impulse conduction in mammalian sinoatrial node. *Am. J. Physiol.* 245:H42–H53.

45. Allessie, M. A., F. I. M. Bonke, and F. J. G. Schopman. 1977. Circus movement in rabbit atrial muscle as a mechanism of tachycardia. III. The "leading circle" concept: A new model of circus movement in cardiac tissue without the involvement of an anatomical obstacle. *Circ. Res.* 41:9–18.

46. Chen, P.-S., N. Shibata, E. G. Dixon, R. O. Martin, and R. E. Ideker. 1986. Comparison of the defibrillation threshold and the upper limit of ventricular vulnerability. *Circulation.* 73:1022–1028.